Title
Non-invasive measurements of breast tissue optical properties using frequency-domain photon migration.

Journal
Philosophical transactions of the Royal Society of London. Series B, Biological sciences, 352(1354)

ISSN
0962-8436

Authors
Tromberg, BJ
Coquoz, O
Fishkin, JB
et al.

Publication Date
1997-06-01

DOI
10.1098/rstb.1997.0047

Non-invasive measurements of breast tissue optical properties using frequency-domain photon migration

BRUCE J. TROMBERG[1], OLIVIER COQUOZ[1], JOSHUA B. FISHKIN[1], TUAN PHAM[1], ERIC R. ANDERSON[2], JOHN BUTLER[3], MITCHELL CAHN[3], JEFFREY D. GROSS[1,3], VASAN VENUGOPALAN[1] AND DAVID PHAM[1]

[1] *Beckman Laser Institute and Medical Clinic, University of California, Irvine, CA 92612–1475, USA*
[2] *EA Photonics, 2515 Fisk Lane, Redondo Beach, CA 90278, USA*
[3] *Department of Surgery, Surgical Oncology, Clinical Cancer Center, UC Irvine Medical Center, 101 The City Drive, Orange, CA 92868, USA*

SUMMARY

A multiwavelength, high bandwidth (1 GHz) frequency-domain photon migration (FDPM) instrument has been developed for quantitative, non-invasive measurements of tissue optical and physiological properties. The instrument produces 300 kHz to 1 GHz photon density waves (PDWs) in optically turbid media using a network analyser, an avalanche photodiode detector and four amplitude-modulated diode lasers (674 nm, 811 nm, 849 nm and 956 nm). The frequency-dependence of PDW phase and amplitude is measured and compared to analytically derived model functions in order to calculate absorption, μ_a, and reduced scattering, μ_s', parameters. The wavelength-dependence of absorption is used to determine tissue haemoglobin concentration (total, oxy- and deoxy- forms), oxygen saturation and water concentration. We present preliminary results of non-invasive FDPM measurements obtained from normal and tumour-containing human breast tissue. Our data clearly demonstrate that physiological changes caused by the presence of small (about 1 cm diameter) palpable lesions can be detected using a handheld FDPM probe.

1. INTRODUCTION

Rapid, accurate determination of tissue optical properties is essential to nearly all aspects of photomedicine, from predicting light dosimetry during therapeutic procedures such as photodynamic therapy (PDT) (Tromberg *et al*. 1995*b*) to interpreting the information content of backscattered or transmitted light during diagnostic studies such as optical mammography. However, the precise relationship between *in vivo* optical properties and tissue physiology is not well understood. Extensive *in vitro* measurements of the optical properties of various tissues have been reported (Cheong *et al*. 1990; Peters *et al*. 1990; Troy *et al*. 1996), but it is likely that these methods do not provide accurate values for tissue optical properties *in vivo*. With the development of quantitative non-invasive diagnostic techniques such as frequency-domain photon migration (FDPM), we expect that a body of work that resolves ambiguities regarding the accuracy and physiological relevance of tissue optical properties will emerge.

In FDPM, the intensity of light incident on an optically turbid sample is modulated at high frequencies (e.g. hundreds of MHz), and the diffusely reflected, transmitted or re-emitted (e.g. fluorescent) signal is measured with a phase-sensitive detector. Intensity-modulated light propagates through multiple-scattering media with a coherent front, forming photon density waves (PDW) (O'Leary *et al*. 1992; Fishkin & Gratton 1993; Tromberg *et al*. 1993). PDW dispersion is highly dependent on the optical properties of the medium (Tromberg *et al*. 1995*a*). Analytical solutions to a photon diffusion equation have been developed that describe the impact of factors such as tissue geometry and boundaries on photon density waves (Arridge *et al*. 1992; Fishkin & Gratton 1993; Haskell *et al*. 1994; Patterson 1995). Exact absorption (μ_a) and reduced scattering (μ_s') parameters are calculated by comparing the measured frequency- or distance-dependent PDW phase and amplitude behaviour to analytically derived nonlinear model functions. When optical properties (μ_s' and μ_a) are recovered for various source wavelengths, the spectral-dependence of absorption can be used to calculate physiologically relevant parameters, such as oxygenated, deoxygenated and total haemoglobin concentration; oxygen saturation; drug concentration; relative blood volume; and water concentration. To calculate these values with high accuracy and precision, tissue scattering and absorption should be separated. Generally, this requires implementation of time- or frequency-domain methods.

Frequency-domain measurements can be broadly grouped into 'multidistance' and 'multifrequency' categories. The former requires sampling diffusely

reflected light signals from several different tissue locations, and the latter employs a single source–detector position and multiple source modulation frequencies (Madsen *et al*. 1994*b*; Tromberg *et al*. 1995). In the case of multifrequency measurements, complete resolution of μ_s' and μ_a is accomplished by analysing PDW dispersion at relatively high modulation frequencies (Tromberg *et al*. 1993, 1995; Haskell *et al*. 1995). We have therefore constructed a 1 GHz portable FDPM device that employs an avalanche photodiode (APD) detector and direct modulation of several (4–8) near-infrared diode lasers (Madsen *et al*. 1994*a*). Modulation is swept from 300 kHz to 1 GHz in less than 1 s, providing rapid multiwavelength (*ca*. 670–960 nm) characterization of most tissues in a single measurement. The instrument is compact and can easily be transported to operating rooms and bedridden patients. By incorporating several near-infrared laser diodes, a number of wavelength-dependent physiological parameters are determined.

This article presents an overview of FDPM instrumentation, data analysis and clinical measurements. One of our long-term goals is to develop FDPM techniques for characterizing normal and malignant breast tissue. Optical methods may provide a functional basis for distinguishing between malignant and benign lesions. In breast tissue, benign conditions such as fibrocystic changes and fibroadenoma occur clinically in 50% of women (Hindle 1990). In the absence of accompanying hyperplasia these do not generally result in an increased risk of breast cancer. However, a majority of surgical biopsies are performed on benign lesions due to the ambiguity of conventional diagnostic methods (e.g. palpation, X-ray mammography, fine needle aspiration) (Hindle 1990; Beam *et al*. 1996). In addition, a substantial number of mammographic studies result in false-negative determinations, particularly for premenopausal patients under 50 years old (Bird *et al*. 1992; Joensuu *et al*. 1994; Kerlikowske *et al*. 1996) and women receiving oestrogen replacement therapy (Laya *et al*. 1996). Collectively, these insufficiencies underscore the need to develop alternative methods that enhance the sensitivity and specificity of breast cancer detection.

2. MATERIALS AND METHODS

(*a*) *Frequency-domain diffusion model*

Frequency-domain methods have been successfully applied to *in vitro* spectroscopy studies of turbid media (Sevick *et al*. 1992; Pogue & Patterson 1994; Fantini *et al*. 1995; Fishkin *et al*. 1995; Tromberg *et al*. 1995). Analytical solutions to the standard diffusion equation (SDE) are typically employed to extract absolute absorption and reduced scattering coefficients from frequency-domain data. The frequency-domain SDE has been estimated to be applicable to the study of homogeneous turbid media with optical properties comparable to biological tissue. It is generally valid for source–detector separations greater than about 1 cm and source modulation frequencies less than about 1 GHz. The use of smaller source–detector separations and higher frequencies may require more sophisticated diffusion expressions, such as the P-1 equation, in order to accurately recover optical properties (Haskell *et al*. 1995; Fishkin *et al*. 1996).

In this work the light source and detector are placed directly on the tissue surface in a reflection geometry. Under these conditions we employ analytical expressions that take the refractive index mismatch at the air/tissue interface into account and assume that the tissue is semi-infinite and homogeneous. The complete 'extrapolated boundary condition' equations describing the phase shift, Φ, and amplitude, A, of photon density waves propagating in semi-infinite media are given elsewhere (Haskell *et al*. 1994).

(*b*) *FDPM instrument*

To reliably calculate absolute absorption (μ_a) and reduced scattering (μ_s') coefficients we must measure the frequency-dependence of photon density wave propagation in tissue. This is given by the PDW phase, Φ, and amplitude, A, at a given source–detector separation, ρ. A portable multilight source, high-bandwidth, FDPM instrument has been developed for this purpose (figure 1). The core component of our FDPM system is a network analyser (Hewlett Packard, model 8753C) that is used to produce modulation swept from 300 kHz to 1 GHz (20 dBm RF output). RF from the network analyser is superimposed on the direct current of up to four different diode lasers (SDL Inc., models 7421, 5420, 5421 and 6321 at 674, 811, 849 and 956 nm, respectively) using individual bias-tees (model 5575A, Picosecond Pulse Labs) and an RF switch (model 8768K, Hewlett Packard). Four, 100 μm diameter gradient-index fibres are used to couple each light source to an 8×8 optical multiplexer (model GP700, DiCon Instruments). An optical tap diverts a portion of the source output (*ca*. 5%) to a 1 GHz PIN diode (New Focus) coupled to the network analyser channel B. This configuration provides a dynamic phase reference and permits real-time compensation for source fluctuations.

Light is launched onto the tissue (or test object) using up to eight unique source fibres, corresponding to eight source positions. An APD (Hamamatsu, model C5658) is used to detect the diffuse optical signal that propagates through the biological tissue. Both the APD and probe end of the source optical fibre are in direct contact with the patient (i.e. a 'semi-infinite medium' measurement geometry). The optical power coupled into the tissue averages approximately 10–30 mW, roughly a factor of 10 below thermal damage threshold levels for fibre-delivered red/NIR (near-infrared) light. Up to eight separate sources can be directed onto up to eight unique measurement positions using the 8×8 optical multiplexer. Measurement time depends on the precision required, the number of sweeps performed and RF/optical switch times. For human subject studies, approximately 0.5 s is used to sweep over the entire 1 GHz band of modulation frequencies. However, total elapsed time for four diodes (two sweeps per diode), data transfer, display and source switching is approximately 40 s. Most components,

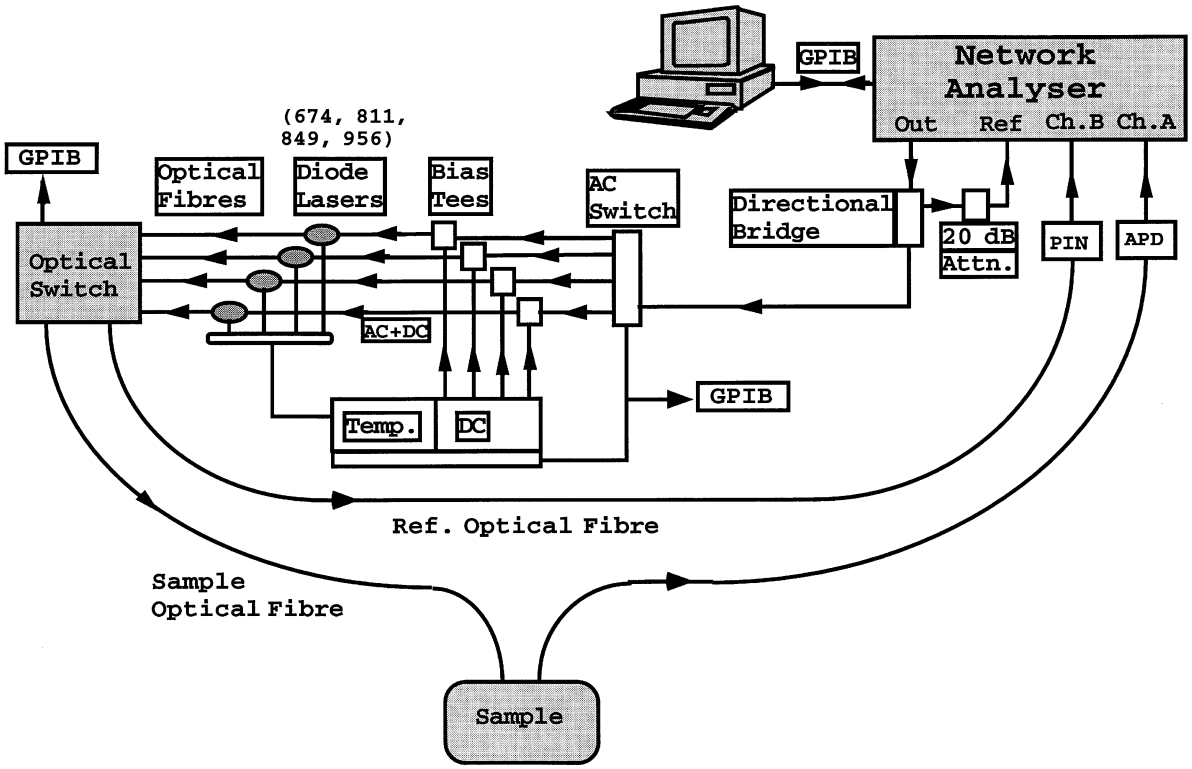

Figure 1. Multiwavelength, multifrequency FDPM instrument.

including the network analyser, RF/optical switches, diode power supplies and temperature of diode mounts are controlled by computer (Macintosh Quadra) using virtual instrument software (LabView, National Instruments). The source–detector separation used for human subject measurements was 2.2 cm.

(*c*) *Instrument calibration*

A measurement of the phase shift of intensity modulated light at source wavelength, λ, propagating through a turbid medium at a given source–detector separation, ρ, can be expressed as follows:

$$\Phi_{\text{measured}}(\mu_a, \mu_s', \rho, \omega) = \Phi_{\text{medium}}(\mu_a, \mu_s', \rho, \omega) + \Phi_{\text{instrument}}(\omega, \lambda), \quad (1)$$

where $\Phi_{\text{measured}}(\mu_a, \mu_s', \rho, \omega)$ is the measured phase shift; $\Phi_{\text{medium}}(\mu_a, \mu_s', \rho, \omega)$ is the actual phase shift caused only by the medium optical properties; and $\Phi_{\text{instrument}}(\omega, \lambda)$ is the 'instrument phase', which depends on the properties of the light source, detector, optical fibres and the electrical response of the phase-sensitive detection system. As $\mu_a(\lambda)$ and $\mu_s'(\lambda)$ are the immediate quantities of interest, an accurate determination of these optical parameters from frequency-domain data requires an analysis of $\Phi_{\text{medium}}(\mu_a, \mu_s', \rho, \omega)$. Thus, we must explicitly determine $\Phi_{\text{instrument}}(\omega, \lambda)$ and subtract this response from $\Phi_{\text{measured}}(\mu_a, \mu_s', \rho, \omega)$ to yield accurate values of $\mu_a(\lambda)$ and $\mu_s'(\lambda)$ from model function fits. Similar arguments can be made for amplitude data (A); however, A_{medium} is determined by evaluating measured and instrument response ratios.

One method for eliminating the instrument response from FDPM data acquired in a macroscopically homogeneous turbid medium is to compare PDW properties measured at two different source–detector separations, ρ and ρ_o (Fantini *et al.* 1994). Assuming that the instrument response at a given source wavelength is constant for separate measurements at ρ and ρ_o, the behaviour of the resulting FDPM data should be entirely reflective of the optical properties of the turbid medium under investigation, and independent of the above mentioned 'instrument response'. This approach works well under macroscopically homogeneous measurement conditions because the frequency-domain SDE assumes that $\mu_a(\lambda)$ and $\mu_s'(\lambda)$ are independent of source–detector separation.

However, in tissues, the assumption that the $\mu_a(\lambda)$ and $\mu_s'(\lambda)$ values are constant throughout the tissue is not necessarily valid. The 'two-distances' measurement technique may compound inaccuracies inherent in applying the SDE (which assumes macroscopic homogeneity) to macroscopically heterogeneous systems. For this reason, we determine optical properties from *in vivo* FDPM data acquired at a single source–detector separation, ρ. Although the application of the SDE to FDPM data acquired at a single ρ may still not be strictly accurate, we assume that the $\mu_a(\lambda)$ and $\mu_s'(\lambda)$ values measured represent an average for the heterogeneous region probed. Using this approach, the degree of tissue heterogeneity can be estimated by evaluating the optical properties at multiple values of ρ. This may be particularly important when characterizing structurally and functionally heterogeneous tissues such as tumours.

To extract $A, \Phi_{\text{medium}}(\mu_a, \mu_s', \rho, \omega)$ from A, $\Phi_{\text{measured}}(\mu_a, \mu_s', \rho, \omega)$ at a single source–detector separation, $\rho, A, \Phi_{\text{instrument}}(\omega, \lambda)$ must be explicitly evaluated (see equation (1)). We account for the

instrument contribution to the measured phase and amplitude by calibrating the FDPM system at each λ on a macroscopically homogeneous, tissue-like reference material of known optical properties. This 'tissue phantom' is cast from flexible silicone, (RTV 615/700, GE corporation) in a 400 ml mould. The optical properties, $\mu_a(\lambda)_{ref}$ and $\mu_s'(\lambda)_{ref}$, of the homogeneous standard are obtained from FDPM data acquired using the 'two-distance' technique. We note from equation (1) that the uncertainties in A, $\Phi_{instrument}(\omega, \lambda)$ must propagate into $A, \Phi_{medium}(\mu_a, \mu_s', \rho, \omega)$. The magnitude of these uncertainties has a direct impact on errors in optical and physiological property calculations.

(*d*) *Human subject measurements and conversion of optical to physiological properties*

We have conducted non-invasive optical property measurements of palpable tumours in two human subjects. Experiments were performed under the guidelines of UC Irvine IRB-approved protocol 95–563. Patient 1 was a 56-year-old postmenopausal female with a single distinct lesion buried approximately 1 cm ($\pm$0.5 cm) beneath the skin surface in the lateral region of the right breast. Histological examination following surgical biopsy revealed a $1.5 \times 2 \times 1$ cm fibroadenoma with ductal hyperplasia (benign tumour). Patient 2 was a 27-year-old premenopausal lactating patient with a similarly sized lesion in the upper outer quadrant of the right breast. Subsequent needle biopsy revealed the presence of a benign fluid-filled cyst, consistent with fibrocystic changes.

Measurements were performed on each patient by gently placing the FDPM probe on both normal and tumour-containing breast. Just enough pressure was applied to ensure optical contact between tissue and probe. Sequential scans of the same location following probe removal and replacement revealed no significant variations in optical properties. Tumour data were acquired for each patient by positioning the probe so that the source and detector ($\rho = 2.2$ cm) bracketed the tumour. Two separate datasets were recorded by rotating the probe through 90 degrees. Normal tissue measurements were acquired from a symmetric site on the opposite, uninvolved breast. Four diode laser sources were used: 674, 811, 849 and 956 nm. As described above, source modulation frequencies ranged from 300 kHz to 1 GHz, and FDPM data were recorded in 5 MHz increments.

Average phase and amplitude values were obtained over this *ca.* 1 GHz bandwidth by performing two multifrequency sweeps per measurement. The uncertainties in $A, \Phi_{measured}(\mu_a, \mu_s', \rho, \omega)$ are the standard deviations from these quantities. Total phase and amplitude error is a combination of the uncertainties in $A, \Phi_{measured}(\mu_a, \mu_s', \rho\ , \omega)$ and $A, \Phi_{instrument}(\omega, \lambda)$ (from calibrating on a macroscopically homogeneous standard phantom) (Fishkin *et al.* 1997). Typical phase and amplitude precision are less than 0.3° and 0.6%, respectively, for signal levels as low as *ca.*–40 dBm and 1 s sweep times.

Phase and amplitude data obtained from FDPM tissue measurements were fitted to semi-infinite model functions (Haskell *et al.* 1994; Fishkin *et al.* 1997) to extract the absolute optical absorption coefficient, μ_a, and the absolute optical reduced scattering coefficient, μ_s', at a given λ and source–detector separation, ρ. Minimization of the χ^2 surface was achieved for simultaneous error-weighted fitting of the Φ and A versus frequency data using a Marquardt–Levenberg algorithm. A tissue refractive index of 1.40 was used in all data fits (Bolin *et al.* 1989). Typical μ_a and μ_s' uncertainties, determined from the χ^2 distribution of phase and amplitude fits, ranged from 0.5–1% of the mean value.

We assume that the chromophores contributing to μ_a in the human subject are principally oxy- and deoxyhaemoglobin, and water (Cope 1991; Sevick *et al.* 1991). The concentration of each component in the tissue is determined from the FDPM measurements of μ_a at three different wavelengths. A system of three equations of the form:

$$\epsilon^{\lambda}_{[Hb]}[Hb] + \epsilon^{\lambda}_{[HbO_2]}[HbO_2] + \epsilon^{\lambda}_{[H_2O]}[H_2O] = \mu^{\lambda}_a, \quad (2)$$

is solved, where $\epsilon^{\lambda}_{[chrom.]}$ is the extinction coefficient (in units of $cm^2\ mol^{-1}$) of a given chromophore at wavelength, λ, and [Hb], [HbO_2], and [H_2O] are respectively the concentration of haemoglobin, oxygenated haemoglobin and water (in units of mol cm^{-3}) in the tissue under study. As measurements of μ_a are made at four different light wavelengths, we use three equations to determine the three unknown quantities [Hb], [HbO_2] and [H_2O]. $\epsilon^{\lambda}_{[Hb]}$, $\epsilon^{\lambda}_{[HbO_2]}$ and $\epsilon^{\lambda}_{[H_2O]}$ are obtained from literature values (Hale & Querry 1973; Cope 1991). For the wavelengths of 674, 811 and 956 nm, the matrix representation of the system of three equations given by equation (2) is:

$$\begin{bmatrix} 6.5783 \times 10^6 & 0.7401 \times 10^6 & 0.0748 \\ 1.8331 \times 10^6 & 2.1539 \times 10^6 & 0.427 \\ 1.5006 \times 10^6 & 3.0486 \times 10^6 & 7.24 \end{bmatrix} \times \begin{bmatrix} [Hb] \\ [HbO_2] \\ [H_2O] \end{bmatrix} = \begin{bmatrix} \mu_a^{674} \\ \mu_a^{811} \\ \mu_a^{956} \end{bmatrix}. \quad (3)$$

Each column of the above matrix contains the extinction coefficients of a given chromophore at each of the above mentioned wavelengths. Each row of the matrix corresponds to a different light wavelength, λ. Multiplication of the above equation by the inverse of the above matrix of extinction coefficients yields values for [Hb], [HbO_2] and [H_2O] in the tissue interrogated by our FPDM instrument. The use of 674, 811 and 956 nm data in a simple 3×3 matrix was found to yield comparable physiological properties to least squares analysis (LSA) using all four wavelengths.

3. RESULTS AND DISCUSSION

To become clinically useful, optical methods should be capable of recording optical and physiological properties with a reasonable degree of spatial resolution. Several groups are close to generating two- and three-dimensional optical property images using a

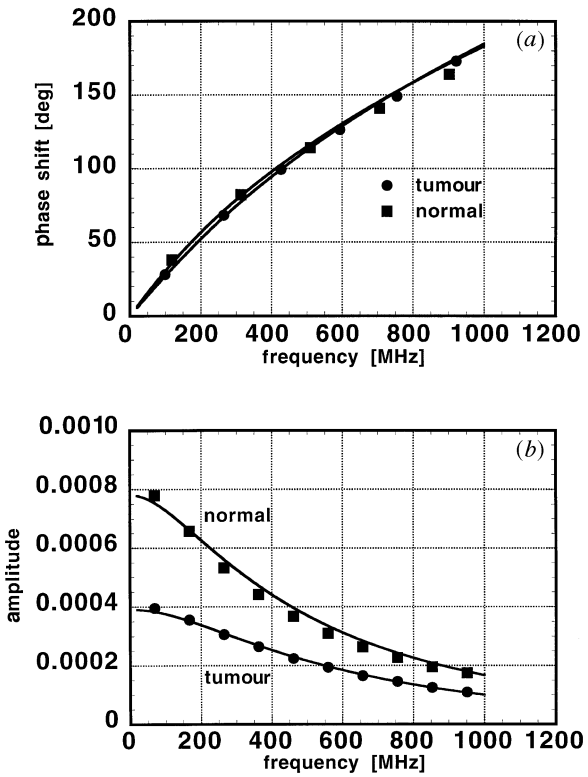

Figure 2. FDPM measurements of phase (*a*) and amplitude (*b*) versus source modulation frequency obtained from normal and tumour sites on patient 1. Source–detector distance = 2.2 cm; $\lambda = 811$ nm. Solid lines are best simultaneous fits to phase and amplitude data from tumour (●) and normal (■) data points, respectively.

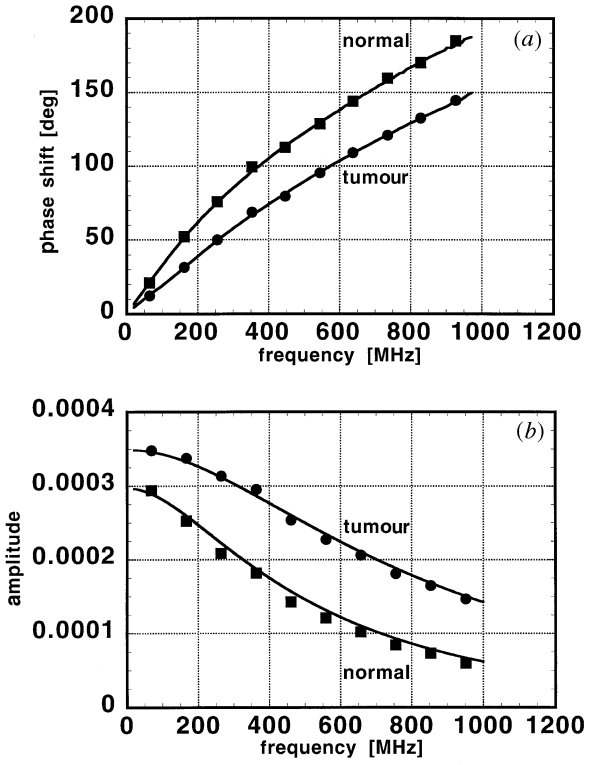

Figure 3. FDPM measurements of phase (*a*) and amplitude (*b*) versus source modulation frequency obtained from normal and tumour sites on patient 2. Source–detector distance = 2.2 cm; $\lambda = 811$ nm. Solid lines are best simultaneous fits to phase and amplitude data from tumour (●) and normal (■) data points, respectively.

variety of technical approaches (Arridge 1995; O'Leary *et al.* 1995; Chang *et al.* 1996; Huabei *et al.* 1996). However, little is known about whether tumours can be identified by optically measured features. In a previous study we characterized optical and physiological properties of large (8–10 cm) subcutaneous adenocarcinoma lesions (abdomen and back) in a human subject (Fishkin *et al.* 1997). These bulky masses provided 'pure' tumour signal, with negligible effect from surrounding normal tissue. Tumour haemoglobin and blood-volume-fraction values ranged from 87–102 μM and 5.2–6.1 %, respectively; approximately two- to fourfold higher than adjacent normal structures. Normal abdominal tissue water content averaged about 11 %; two- to fivefold less than tumours.

In this preliminary two-patient study we examined whether small palpable breast lesions could be detected non-invasively using the same handheld FDPM probe. Each patient received surgical or needle biopsies following FDPM. Conventional histology was then compared to non-invasive optical measurements. Although it was not possible to precisely determine the relative contributions of size, absorption and scattering to the measured signals, our results clearly show that buried lesions can substantially perturb normal tissue properties. Much work remains to assess different tissue types, assign FDPM-measured properties to tumours and correlate optical measurements with conventional techniques.

Results of 811 nm FDPM measurements are shown for patients 1 and 2 in figures 2 and 3, respectively. Raw data reveal clear differences between normal and tumour sites. Normal tissue scans were obtained from the symmetric position on the opposite breast. In the case of patient 1 (figure 2), tissue differences are more obvious in amplitude (figure 2*b*) rather than phase (figure 2*a*) data. For this reason we have employed a technique for simultaneously fitting phase and amplitude to FDPM nonlinear model functions. Optical properties obtained from these fits are shown as a function of wavelength in figures 4 and 5.

Figures 4*a* and 5*a* show that absorption values obtained from tumour-containing tissue are consistently higher than normal for each patient. Although the magnitude of the absorption change is greater for patient 2, it is impossible to determine whether this is a consequence of intrinsic lesion properties or differences in size and depth. In patient 1, tumour absorption increases slightly from 674 to 811 nm, then drops at 849 nm. This behaviour is reversed for normal and tumour tissue in patient 2.

Physiological differences between patients are further amplified by results of reduced scattering coefficient, μ_s', calculations. Figures 4*b* and 5*b* show that μ_s' decreases gradually with increasing wavelength. Tumour values are consistently higher for patient 1 than for normals, while the opposite is observed for patient 2. Histology revealed a fibroadenoma (approximately $1 \times 1.5 \times 2$ cm^3 and 1 cm deep) with mild ductal

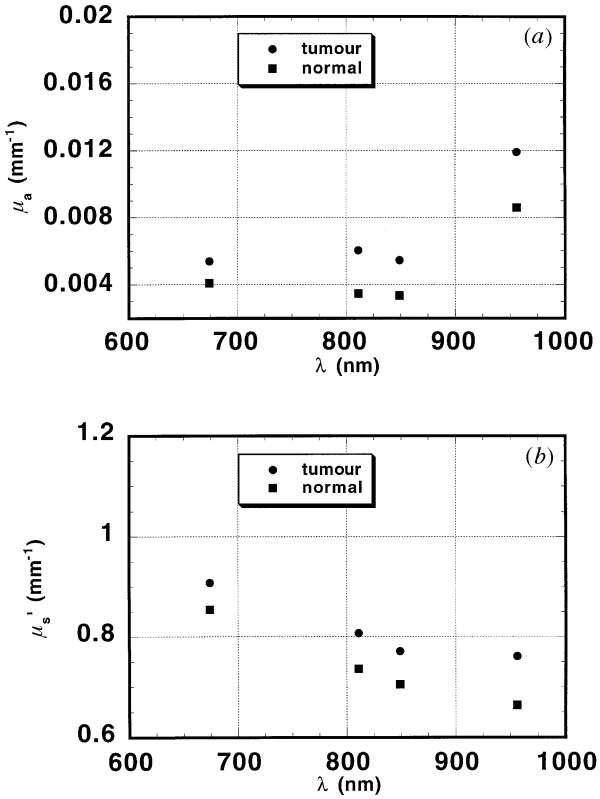

Figure 4. Absorption coefficient, μ_a (*a*) and reduced scattering coefficient μ_s' (*b*) versus source wavelength for normal and malignant breast tissue, patient 1. Values calculated from best simultaneous fits of model functions to phase and amplitude data shown in figure 3.

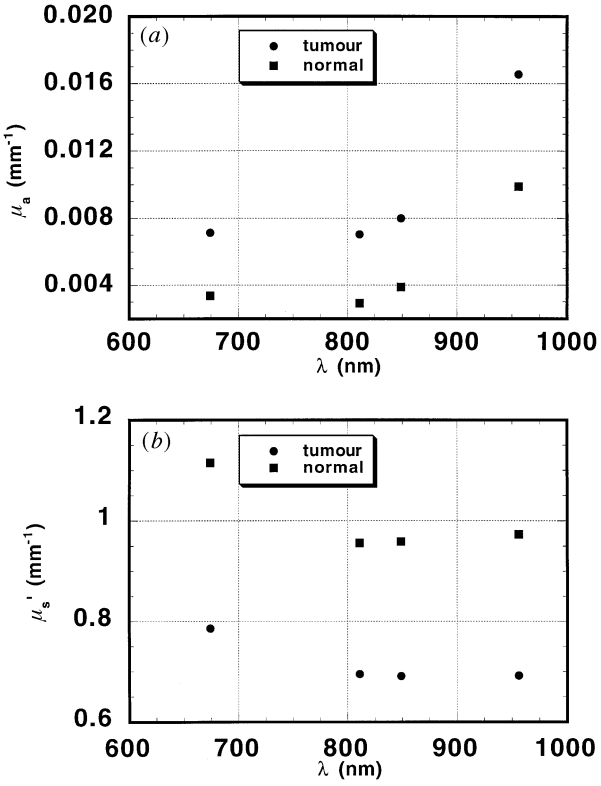

Figure 5. Absorption coefficient, μ_a (*a*) and reduced scattering coefficient μ_s' (*b*) versus source wavelength for normal and malignant breast tissue, patient 2. Values calculated from best simultaneous fits of model functions to phase and amplitude data shown in figure 4.

hyperplasia, and an acellular, fluid-filled cyst for patients 1 and 2, respectively. Scattering values are compatible with histology reports as lower μ_s' is expected for fluid-filled structures (i.e. fluid-filled cyst), and increased scattering should occur in the case of fibrotic tissue (i.e. fibroadenoma). Normal tissue scattering is 1.3- to 1.4-fold higher for the pre- versus postmenopausal patient. It is likely that these differences are a consequence of the fact that premenopausal, highly glandular tissue has substantial structural complexity whereas postmenopausal breast is dominated by low water content adipose.

Physiological properties extracted from μ_a values are summarized in figure 6. Total and oxyhaemoglobin levels are approximately twofold higher in tumour versus normal tissue for both patients. Deoxyhaemoglobin contrast persists for patient 2 but does not appear for patient 1. As a result, differences in normal versus tumour tissue oxygen saturation (SaO_2) are greater for patient 1 (68 % versus 79 %, respectively) than for patient 2 (66 % versus 74 %). SaO_2 values are larger in tumour-containing tissue, perhaps due to higher blood flow and lower oxygen extraction in regions probed by FDPM measurements. This observation is consistent with the view that benign fibrotic and cystic tumours are not likely to display marked hypoxic zones, a characteristic that is expected to be unique to malignant transformations. Normal SaO_2values are comparable for both patients (68 % and 66 % for patients 1 and 2, respectively).

Tissue water concentration is also displayed in figure 6. It is difficult to confirm the accuracy of these values because they are based on pure water extinction coefficients (as opposed to protein-bound forms) at 25 °C and least squares calculations, which do not take into account the contribution of fat to the 956 nm signal. Nevertheless, all results fall within the 11.4 % to 30.5 % range given in the literature for percentage water in human fatty adipose tissue (Duck 1990). In addition, our data make sense in the context of what is known about patient physiology. For example, premenopausal lactating breast tissue has substantially higher water content than postmenopausal adipose tissue (17 % versus 12 %; where 100 % is about 55 M). The presence of a fluid-filled tumour elevates the percentage water from 17 to 21 % in patient 2, and the fibroadenoma does not affect patient 1. One might expect that increases in total tissue haemoglobin would lead to concomitant elevations in water content (blood is mostly water). However, in the case of patient 1, tumour haemoglobin goes up and water remains constant. Assuming that tissue consists of blood and matrix compartments, a reduction in matrix water would compensate for the lack of an overall tissue water increase. Histologic examination of fibroadenomas showing dense fibrotic zones surrounding shrunken glandular structures provides additional support for this concept. Further confirmation is provided by our observation of elevated fibroadenoma μ_s' values (figure 4*b*).

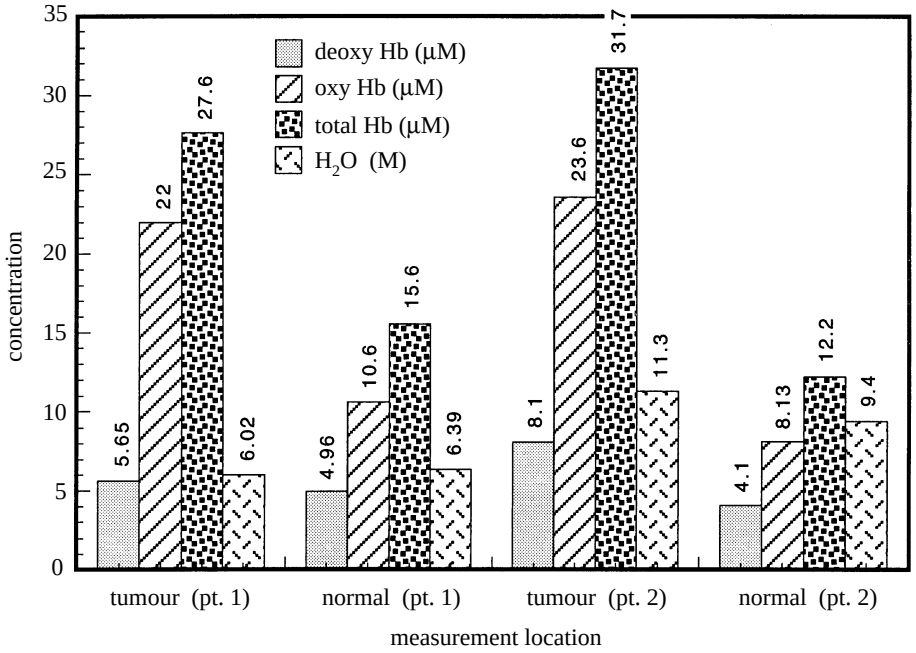

Figure 6. Haemoglobin (μM, deoxy-, oxy- and total) and water (M) concentrations for normal and tumour breasts, patients 1 and 2, calculated from wavelength-dependent μ_a values.

4. CONCLUSIONS

We have developed a multiwavelength, multi-frequency, handheld FDPM probe for non-invasive characterization of tissue optical properties. Unique features include the ability to measure photon density wave phase and amplitude, and simultaneously fit data to non-linear, frequency-dependent model functions. Optical and physiological properties are calculated for distinct source–detector separations by comparing the tissue response to a calibrated standard. Results of preliminary studies in human breast tissue show that FDPM is sensitive to absorption and scattering changes induced by the presence of small (about 1 cm diameter), palpable lesions. Although neither of the two patients in this study had malignant tumours, optical and physiological properties of benign lesion-embedded sites were clearly observed. Considerable work remains to explicitly assign absorption and scattering parameters to buried lesions and to clearly demonstrate whether this approach has utility in clinical diagnostics. We are currently in the process of acquiring additional data from patients, which we expect will provide much-needed insight into optical and physiological characteristics of benign, malignant and non-neoplastic tumours.

This work was made possible, in part, through access to the Laser Microbeam and Medical Program (LAMMP) and the Clinical Cancer Center Optical Biology Shared Resource at the University of California, Irvine. These facilities are supported by the National Institutes of Health under grants RR-01192 and CA-62203, respectively. Beckman Laser Institute programmatic support was provided by the Department of Energy (DOE # DE-FG03-91ER61227), and the Office of Naval Research (ONR # N00014-91-C-0134). O. C. wishes to acknowledge the Swiss National Science Foundation and the Cancer Research Switzerland (BIL KFS 205-9-1995). B. J. T. acknowledges the National Institutes of Health (GM50958) and the California Breast Cancer Research Program. We are grateful to Natasha Shah and Jenny Espinoza for their contributions to this research.

REFERENCES

Arridge, S. R., Cope, M. & Delpy, D. T. 1992 Theoretical basis for the determination of optical path lengths in tissue: temporal and frequency analysis. *Phys. Med. Biol.* **37**, 1531–1560.

Arridge, S. R. 1995 Photon-measurement density functions. Analytical forms (medical imaging application). *Appl. Opt.* **34**, 7395–7409.

Beam, C. A., Layde, P. M. & Sullivan, D. C. 1996 Variability in the interpretation of screening mammograms by US radiologists. Findings from a national sample. *Archs Intern. Med.* **156**, 209–213.

Bird, R., Wallace, T. W. & Yankaskas, B. C. 1992 Analysis of cancers missed at screening mammography. *Radiology* **184**, 613–617.

Boas, D. A., O'Leary, M. A., Chance, B. & Yodh, A. G. 1993 Scattering and wavelength transduction of diffuse photon density waves. *Phys. Rev. E* **47**, R2999–R3002.

Bolin, F. P., Preuss, L. E., Taylor, R. C. & Ference, R. J. 1989 Refractive index of some mammalian tissues using a fiber optic cladding method. *Appl. Opt.* **28**, 2297–2303.

Chang, J., Graber, H. L., Barbour, R. L. & Aronson, R. 1996 Recovery of optical cross-section perturbations in dense-scattering mediaby transport-theory-based imaging operators and steady-state simulated data. *Appl. Opt.* **35**, 3963–3978.

Cheong, W. F., Prahl, S. A. & Welch, A. J. 1990 A review of the optical properties of biological tissues. *IEEE J. Quantum Electron.* **26**, 2166–2185.

Cope, M. 1991 The development of a near infrared spectroscopy system and its application for non invasive monitoring of cerebral blood and tissue oxygenation in the newborn infant. Ph.D. thesis, University of London, Department of Medical Physics and Bioengineering, University College London.

Duck, F. A. 1990 *Physical properties of tissue*, pp. 320–328. London: Academic Press.

Fantini, S., Franceschini, M. A., Fishkin, J. B., Barbieri, B. & Gratton, E. 1994 Quantitative determination of the absorption spectra of chromophores in strongly scattering media: a light-emitting-diode based technique. *Appl. Opt.* **33**, 5204–5213.

Fishkin, J. B., Coquoz, O., Anderson, E. A., Brenner, M. & Tromberg, B. J. 1997 Frequency-domain photon migration measurements of normal and malignant tissue optical properties in a human subject. *Appl. Opt.* **36**, 10–20.

Fishkin, J. B., Fantini, S., van de Ven, M. J. & Gratton, E. 1996 Gigahertz photon density waves in a turbid medium: theory and experiments. *Phys. Rev.* E **53**, 2307–2319.

Fishkin, J. B. & Gratton, E. 1993 Propagation of photon density waves in strongly scattering media containing an absorbing semi-infinite plane bounded by a straight edge. *J. Opt. Soc. Am.* A **10**, 127–140.

Fishkin, J. B., So, P. T.-C., Cerussi, A. E., Fantini S., Franceschini, M. A. & Gratton, E. 1995 Frequency-domain method for measuring spectral properties in multiple-scattering media: methemoglobin absorption spectrum in a tissuelike phantom. *Appl. Opt.* **34**, 1143–1155.

Hale, G. M. & Querry, M. R. 1973 Optical constants of water in the 200 nm to 200 m wavelength region. *Appl. Opt.* **12**, 555–563.

Haskell, R. C., Svaasand, L. O., Tsay, T.-T., Feng, T.-C., McAdams, M. S. & Tromberg, B. J. 1994 Boundary conditions for the diffusion equation in radiative transfer. *J. Opt. Soc. Am.* A **11**, 2727–2741.

Hindle, W. H. 1990 *Breast disease for gynecologists*, pp. 155–171. New Jersey: Prentice Hall.

Huabei, J., Paulsen, K. D., Osterberg, U. L., Pogue, B. W. *et al.* 1996 Optical image reconstruction using frequency-domain data: simulations and experiments. *J. Opt. Soc. Am.* A **13**, 253–266.

Joensuu, H., Asola, R., Holli, K., Kumpulainen, E., Nikkanen, V. & Parvinen, L. M. 1994 Delayed diagnosis and large size of breast cancer after a false negative mammogram. *Eur. J. Cancer* **30**, 1299–1302.

Kerlikowske, K., Grady, D., Barclay, J., Sickles, E. A. & Ernster, V. 1996 Effect of age, breast density, and family history on the sensitivity of first screening mammography. *J. Am. Med. Ass.* **276**, 33–38.

Laya, M. B., Larson, E. B., Taplin, S. H. & White, E. 1996 Effect of estrogen replacement therapy on the specificity and sensitivity of screening mammography. *J. Natn. Cancer Inst.* **88**, 643–649.

Madsen, S. J., Anderson, E. R., Haskell, R. C. & Tromberg, B. J. 1994*a* A portable, high-bandwidth frequency-domain photon migration instrument for tissue spectroscopy. *Optics Lett.* **19**, 1934–1936.

Madsen, S. J., Wyss, P., Svaasand, L. O., Haskell, R. C., Tadir, Y. & Tromberg, B. J. 1994*b* Determination of the optical properties of human uterus using frequency-domain photon migration and steady-state techniques. *Phys. Med. Biol.* **39**, 1191–1202.

O'Leary, M. A., Boas, D. A., Chance, B. & Yodh, A. G. 1995 Experimental images of heterogeneous turbid media by frequency-domain diffusing-photon tomography. *Optics Lett.* **20**, 426–428.

O'Leary, M. A., Boas, D. A., Chance, B., & Yodh, A. G. 1992 Refraction of diffuse photon density waves. *Phys. Rev. Lett.* **69**, 2658.

Patterson, M. S. 1995 Noninvasive measurements of tissue optical properties: current status and future prospects. Comments on molecular and cellular biophysics. *Comments Modern Biol.* A **8**, 387–417.

Patterson, M. S., Moulton, J. D., Wilson, B. C., Berndt, K. W. & Lakowicz, J. R. 1991 Frequency-domain reflectance for the determination of the scattering and absorption properties of tissue. *Appl. Opt.* **30**, 4474–4476.

Peters, V. G., Wyman, D. R., Patterson, M. S. & Frank, G. L. 1990 Optical properties of normal and diseased human breast tissues in the visible and near infrared. *Phys. Med. Biol.* **335**, 1317–1334.

Pogue, B. W. & Patterson, M. S. 1994 Frequency-domain optical absorption spectroscopy of finite tissue volumes using diffusion theory. *Phys. Med. Biol.* **39**, 1157–1180.

Sevick, E. M., Chance, B., Leigh, J., Nioka, S. & Maris, M. 1991 Quantitation of time- and frequency-resolved optical spectra for the determination of tissue oxygenation. *Anal. Biochem.* **195**, 330–351.

Tromberg, B. J., Haskell, R. C., Madsen, S. J. & Svaasand, L. O. 1995*a* Characterization of tissue optical properties using photon density waves. *Comments Molec. Cell. Biophys.* **8**, 359–386.

Tromberg, B. J., Svaasand, L. O., Fehr, M. K., Madsen, S. J., Wyss, P., Sansone, B. & Tadir, Y. 1995 A mathematical model for light dosimetry in photodynamic destruction of human endometrium. *Phys. Med. Biol.* **40**, 1–15.

Tromberg, B. J., Svaasand, L. O., Tsay, T.-T. & Haskell, R. C. 1993 Properties of photon density waves in multiple-scattering media. *Appl. Opt.* **32**, 607–616.

Troy, T. L., Page, D. L. & Sevick-Muraca, E. M. 1996 Optical properties of normal and diseased breast tissue: prognosis for optical mammography. *J. Biomedical Optics* **1**, 342–355.